Title

Chromatin Kinases Act on Transcription Factors and Histone Tails in Regulation of Inducible Transcription

Journal

Molecular Cell, 64(2)

ISSN

1097-2765

Authors

Josefowicz, Steven Z
Shimada, Miho
Armache, Anja
et al.

Publication Date

2016-10-01

DOI

10.1016/j.molcel.2016.09.026

Peer reviewed

HHS Public Access

Author manuscript

Mol Cell. Author manuscript; available in PMC 2017 October 20.

Published in final edited form as:

Mol Cell. 2016 October 20; 64(2): 347–361. doi:10.1016/j.molcel.2016.09.026.

Chromatin kinases act on transcription factors and histone tails in regulation of inducible transcription

Steven Z. Josefowicz[1,*,#,†], **Miho Shimada**[2,*], **Anja Armache**[1], **Charles H. Li**[1], **Rand M. Miller**[3], **Shu Lin**[4], **Aerin Yang**[5], **Brian D. Dill**[6], **Henrik Molina**[6], **Hee-Sung Park**[5], **Benjamin A. Garcia**[4], **Jack Taunton**[3], **Robert G. Roeder**[2,#], and **C. David Allis**[1,#]

[1]Laboratory of Chromatin Biology and Epigenetics, The Rockefeller University, New York, NY 10065, USA

[2]Laboratory of Biochemistry and Molecular Biology, The Rockefeller University, New York, NY 10065, USA

[3]Department of Cellular and Molecular Pharmacology, University of California, San Francisco, CA 94158, USA

[4]Epigenetics Program, Department of Biochemistry and Biophysics, University of Pennsylvania, Philadelphia, PA 19104, USA

[5]Department of Chemistry, Korea Advanced Institute of Science and Technology, Daejeon 305-701, Korea

[6]Proteomics Resource Center, The Rockefeller University, New York, NY 10065, USA

Summary

The inflammatory response requires coordinated activation of both transcription factors and chromatin to induce transcription for defense against pathogens and environmental insults. We sought to elucidate connections between inflammatory signaling pathways and chromatin through genomic foot-printing of kinase activity and unbiased identification of prominent histone phosphorylation events. We identified H3 serine 28 phosphorylation (H3S28ph) as the principal stimulation-dependent histone modification and observed its enrichment at induced genes in mouse macrophages stimulated with bacterial lipopolysaccharide. Using pharmacological and

[#]Corresponding author: Steven Z. Josefowicz: The Rockefeller University, Allis Lab, Box #78, 1230 York Avenue, New York, NY 10065, USA. sjosefowicz@gmail.com; C. David Allis: The Rockefeller University, Allis Lab, Box #78, 1230 York Avenue, New York, NY 10065, USA. C.David.Allis@rockefeller.edu; Robert G. Roeder: The Rockefeller University, Roeder Lab, Box #166, 1230 York Avenue, New York, NY 10065, USA. Robert.Roeder@rockefeller.edu.

[*]Co-first author

[†]Lead contact

Author Contributions. S.Z.J. designed and performed ChIP-seq, RNA-seq, flow cytometry, genomics analysis, and cellular stimulation-based assays together with A.A. and C.H.L. under the supervision of C.D.A and with input from M.S. and R.G.R. M.S. designed and performed biochemical and *in vitro* transcription assays with input and support from S.Z.J. under the supervision of R.G.R. S.L., H.M., B.A.G., and B.D.D. performed mass spectrometry experiments and data analysis. H.P. and A.Y. generated synthetic histone H3 reagents. R.M.M. and J.T. developed and tested RMM-64 and provided input on the use of chemical agents. S.Z.J and C.D.A. wrote the paper with contributions and input from all authors.

genetic approaches, we identified mitogen- and stress-activated protein kinases (MSKs) as primary mediators of H3S28ph in macrophages. Cell-free transcription assays demonstrated that H3S28ph directly promotes p300/CBP-dependent transcription. Further, MSKs can activate both signal-responsive transcription factors and the chromatin template with additive effects on transcription. Specific inhibition of MSKs in macrophages selectively reduced transcription of stimulation-induced genes. Our results suggest that MSKs incorporate upstream signaling inputs and control multiple downstream regulators of inducible transcription.

eTOC blurb

Josefowicz et al. demonstrate that MSK1/2 coordinately activate both transcription factors and the chromatin template via histone phosphorylation. MSKs thereby regulate rapid transcription of inflammatory genes in response to pathogen sensing. In general, chromatin kinases may represent a nexus of signaling inputs controlling multiple regulators of inducible transcription.

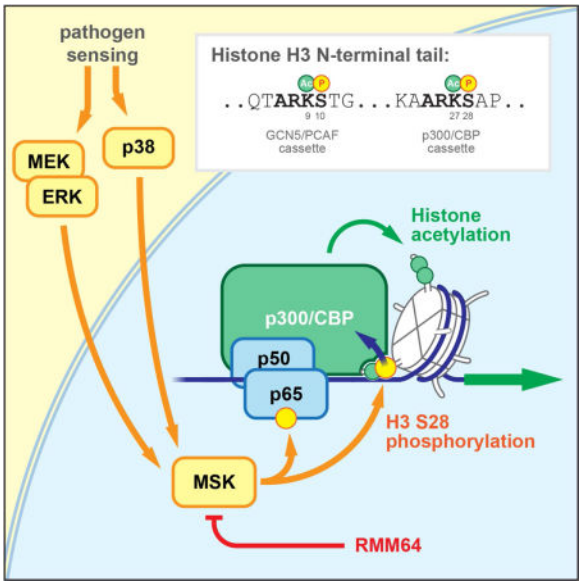

Introduction

Cells responding to environmental signals rapidly and selectively alter gene expression. These changes require the coordinated activity of DNA-binding transcription factors, chromatin regulatory factors, and the general transcription machinery. Innate immune cell recognition of pathogen components represents an archetypal rapid cellular response, in which speed and scope of selective transcription are critical for host organism survival. Induced activation and binding of signal-responsive transcription factors and changes in chromatin features are characteristic of inflammatory gene induction. For example, preexisting chromatin accessibility and histone acetylation and collaboration between signal-responsive transcription factors and chromatin remodelers can determine the level and kinetics of gene induction (Bhatt et al., 2012; Hargreaves et al., 2009; Ostuni et al., 2013; Ramirez-Carrozzi et al., 2009). Beyond the activation of transcription factors, signaling

pathways have potential to directly regulate chromatin characteristics, such as histone modifications and chromatin accessibility, thereby altering transcription.

Cellular stimulation commonly leads to the activation of downstream nuclear and chromatin-associated kinases. While the classical view of transcription regulation by signaling inputs is through the phosphorylation of DNA-binding transcription factors, select kinase pathways signal to chromatin through histone phosphorylation, which serves as a rapid and reversible mechanism by which environmental inputs can affect chromatin processes (Baek, 2011; Cheung et al., 2000). Relationships between these two categories of phosphorylation events remain unclear. Initial studies described histone phosphorylation as a feature of cellular stimulation and linked growth factor signaling to rapid and transient phosphorylation of serine residues in the N-terminal tail of histone H3 (Mahadevan et al., 1991). Further studies revealed the relevance of histone phosphorylation in cell cycle control and mitosis, repair of DNA damage, apoptosis, and transcription (Cheung et al., 2000; Lo et al., 2000). Kinases MSK1/2 were highlighted as integrators of both p38 and ERK signaling with the ability to phosphorylate histone H3 (Thomson, 1999). More recently, MSK1/2 activity and phosphorylation of either H3S10 or H3S28 has been linked to the transcription of immediate-early genes during the fibroblast stress-response (Drobic et al., 2010; Sawicka et al., 2014). Despite involvement in several biological processes, the functions and direct activity of histone phosphorylation are poorly understood.

H3 tail phosphorylation occurs prominently within a repeated amino acid sequence, Ala-Arg-Lys-Ser (ARKS). These motifs contain the lysine residues K9 and K27, which have important regulatory function, with their acetylation or methylation instructing chromatin activation or repression, respectively. Given the similar sequence context of H3S10 and H3S28, it has been unclear whether these phosphorylation events have distinct roles in chromatin regulation. Overall, as a histone modification class, phosphorylation has considerable potential to alter the biophysical character of chromatin and the recruitment of regulatory factors. Here, we sought to identify the major histone phosphorylation events during an archetypal cellular stimulation to inform focused studies on histone phosphorylation pathways, function, and mechanism of action. Our results highlight the dual role of the chromatin-associated kinases (MSK1/2) in the activation of both transcription factors and the chromatin template and reveal a direct, positive activity of H3S28ph on p300/CBP-dependent transcription. Use of pharmacologic approaches to study the function of MSK1/2 during the macrophage response to pathogen sensing demonstrates a selective role for these chromatin-associated kinases in inducible transcription and highlights their potential as drug targets.

Results

Dynamic regulation of histone phosphorylation during macrophage stimulation

To identify potential mechanisms controlling inducible transcription, we focused on the intersection of kinase pathways and chromatin regulation during cellular stimulation. To avoid complications due to mitotic histone phosphorylation, we took advantage of primary macrophages as being post-mitotic. We hypothesized that unbiased identification and foot-printing of principal histone phosphorylation events would indicate relevant kinase activity

and biologically important mechanisms controlling rapid and robust gene expression in cells responding to stimulation.

With the goal of characterizing kinase activity on chromatin during the mouse bone marrow derived macrophage (BMDM) inflammatory response to lipopolysaccharide (LPS) we assessed the scope and kinetics of specific histone phosphorylation events using several complementary approaches. For unbiased determination of histone phosphorylation events, we biochemically purified histone proteins from macrophages throughout the stimulation time course and quantified residue-specific phosphorylation by mass spectrometry (MS). We focused attention on dynamic phosphorylation of serine residues within two regulatory cassettes in the N-terminal tail of H3, H3S10ph and H3S28ph. Histone tail acetylation at these repeated ARKS motifs is mediated by the transcription co-activators GCN5 (H3K9/K14) and p300/CBP (H3K18/K23/K27) (Jin et al., 2011). High-sensitivity quantification was achieved through parallel analysis of TiO_2-bead enriched phospho-peptides and input histone peptides (Figure 1B). Our MS approach identified H3S10 and H3S28 as the most abundant histone phosphorylation events detected in stimulated samples. Interestingly, we observed preexisting levels of H3S10ph and only a moderate increase after stimulation (Figure 1C). Due to the proximity of the S28 residue to the H3.3 histone variant-specific S31 residue, we were able to quantify the enrichment of H3S28ph on both H3.1/2 and H3.3, the latter variant being associated with dynamic chromatin. In contrast to H3S10ph, we observed substantial increases in H3S28ph upon stimulation on H3.1/2 and an increase from undetectable levels to 0.8% of total, on the H3.3 variant (Figure 1C). Phosphorylation of H3T3 or H3T6 was below or near the detection limit under all conditions (Figure 1C). Global levels of histone post-translational modifications other than phosphorylation events were not observed to change noticeably between resting and stimulated conditions (data not shown and Figure 1D).

Western blot analysis also demonstrated dynamic stimulation-responsive regulation of both H3S10ph and H3S28ph, but minimal to no change in global levels of other histone post-translational modifications including H3K27ac (Figure 1D, S1A). While H3S10ph and H3S28ph are abundant in mitotic cells, flow cytometry approaches assured that BMDM were post-mitotic (Figure S1B). Further, these techniques allowed for quantitative, single-cell analysis of histone phosphorylation during the LPS response and revealed a population-level increase in H3S28ph (Figure 1E, Figure S1C). Confocal immunofluorescence microscopy similarly established H3S28ph as a dominant stimulation-dependent histone phosphorylation event, and highlighted its euchromatic localization (Figure S1D). Thus, H3S28ph is a prominent, dynamically regulated histone phosphorylation event during the macrophage response to LPS.

Given the stimulation-dependent induction of H3S28ph, we hypothesized that it might function in rapid transcription of early inflammatory genes. Consistent with this hypothesis, we found through ChIP-sequencing (ChIPseq) approaches that H3S28ph rapidly accumulates at the 5′-end of the most highly induced inflammatory genes (336 genes, Supplementary table 1), but not at non-expressed genes (Figure 1F–G). Consistent with observation of minimal stimulation-dependent induction of H3S10ph by MS/MS (Figure 1C), western blot (Figure 1D), flow cytometry (Figure S1C), and confocal

immunofluorescence microscopy (Figure S1D), we did not observe enrichment of H3S10ph comparable to H3S28ph at LPS-induced genes (Figure S1E).

Stimulation-dependent enrichment of H3S28ph at LPS-activated gene transcription start sites (TSS) and enhancers were correlated (Figure S1F–G) and reached peak levels at 30′ before gradually declining through 240′ post-stimulation (Figure 1H–I, Figure S1H–I). We next sought to more thoroughly characterize the association of H3S28ph with diverse categories of LPS-activated chromatin based on enhancer type (Ostuni et al., 2013) and transcription kinetics (Bhatt et al., 2012). Notably, we found that rapidly activated enhancers and rapidly transcribed genes are associated with early elevated levels of H3S28ph, while genes with peak transcription at two hours or later have either delayed or absent H3S28ph enrichment (Figure S1I–J). Latent enhancers characterized by de novo, stimulation-dependent acquisition of H3K4me1, Pu.1, and H3K27ac, as well as delayed kinetics in stimulus-induced transcription factors (Ostuni et al., 2013) also demonstrated delayed and reduced H3S28ph (Figure S1I), likely due to delays in chromatin accessibility and transcription factor and kinase recruitment. Interestingly, while H3S28ph levels decline at specific genomic loci and globally after one hour, quantification by ChIP-seq and flow cytometry indicates that above-baseline H3S28ph levels are maintained beyond four hours (Figure S1H–I, K). Together, these data indicate that LPS-stimulation of macrophages results in parallel signaling directly to H3S28 in chromatin, specifically targeting genomic loci critical for the rapid response to stimulus.

Phosphorylation of H3S28 at lineage-specific and stimulation-responsive chromatin

We next sought to further characterize the genes and chromatin regions associated with H3S28ph. H3S28ph was positively correlated with LPS-dependent fold-increase in transcription ($p<0.0001$) but not overall expression level transcriptome-wide ($p=0.063$), indicating a specificity for environmental-response genes rather than constitutively expressed genes (Figure S2A–B). Consistent with this, H3S28ph was not induced at constitutively expressed housekeeping genes, including those encoding β-Tubulin and RPS2 (Figure 2A), while it increased following LPS-stimulation at a number of inflammatory genes, including *Ifnb1*, *Il27*, *Cxcl10*, *Tnf*, and *Il12* (Figure 2B). We further established the association of H3S28ph with LPS-response genes through unbiased gene ontology analysis of gene-annotated H3S28ph enriched regions; the most enriched gene ontology category was “regulation of cytokine production” (p-value=1×10^{-180}). Further, we empirically identified a threshold for high-level H3S28ph around TSS regions (Figure 2C) and find that these top 391 H3S28ph genes are induced on average 11.8-fold one hour after LPS stimulation (Figure 2D).

To better understand the biological context, cofactors, and selectivity of H3S28ph during the macrophage response to LPS, we queried H3S28ph chromatin regions for enrichment of transcription factor motifs. We identified highly significant motif enrichment for macrophage lineage-determining transcription factors (PU.1, CEBPα) and environmental response factors (NF-κB, ELK1, RELA, NFKB1, CREB1, AP1) in regulatory DNA elements with high levels of H3S28ph, as compared to regulatory DNA lacking H3S28ph. Motifs for general factors not specifically engaged in the macrophage response to LPS (TBP,

CTCF, REST) were equally represented in regulatory elements with and without H3S28ph enrichment (Figure 2E. Figure S2C–D). Therefore, H3S28ph is induced at both macrophage lineage-specific and stimulation-responsive regulatory elements during LPS-stimulation. Consistent with a role for NF-κB in the targeting of H3S28ph, and suggestive of a role for MAPK signaling, we found that RelA and MAPK-dependent genes (Tong et al., 2016) were further enriched for H3S28ph when compared to other LPS-induced genes (Figure 2F).

Levels of H3S28ph peaked early (30′–60′) at the promoters and enhancers of LPS-induced genes, while global levels of H3S28ph remained elevated four hours after LPS stimulation (Figure S1). To explain this we characterized the genomic distribution of H3S28ph at early and late time points. This analysis revealed that while H3S28ph levels decreased at discrete regions around promoters and enhancers, large chromosome loop boundaries (Dowen et al., 2014) and intervening domains maintained high levels of H3S28ph four hours after stimulation. We found that H3S28ph was enriched within looped chromatin domains defined by conserved CTCF and Cohesin binding sites that contained LPS-induced genes, such as *Tnfaip3* and *Ehd1*, but not in neighboring domains devoid of stimulation responsive chromatin (Figure S2E–F). It is also possible that some changes in histone phosphorylation could occur within repetitive elements or other difficult to analyze sequence. Regardless, this rapid delineation of chromatin domains by H3S28ph is a unique feature of stimulation-responsive chromatin and may feature to alter the biophysical characteristics and accessibility of these domains, enabling their dynamic regulation.

MSKs signal to chromatin at inflammatory response genes

To identify and study the kinase(s) responsible for H3S28ph during the LPS-stimulation, we chose two complementary approaches, siRNA and small-molecule inhibitors. Multiple kinases have been reported to phosphorylate H3S28 in various cell types, most prominently MSK and RSK paralogs (Baek, 2011). siRNA treatment resulted in kinase-specific reduction in mRNA and protein levels and a commensurate decrease in H3S28ph in the case of MSK1 and MSK2 (alone and in combination), but not RSK2 (Figure S3A–B). These kinase knockdown experiments indicate that MSK kinases are predominantly responsible for LPS-induced phosphorylation of H3S28.

To evaluate the effects of more complete kinase loss-of-function with precise temporal control, we utilized small-molecule MSK inhibitors. To control for potential off-target effects, we used two structurally unrelated inhibitors targeting the MSK N- and C-terminal kinase domains (NTD and CTD), respectively (Figure 3A). SB747651A is a potent inhibitor of the AGC-family MSK NTD, but interpretation of its cellular effects may be confounded by inhibition of a number of other AGC kinases in the same pathway, including RSK1/2, PKA, PKB/Akt and PKC (Naqvi et al., 2012). Thus, we developed RMM-64, a reversible covalent inhibitor that inhibits the MSK CTD by targeting a cysteine residue that is absent in all off-target AGC kinases (Figure 3B, Figure S3C–E). RMM-64 retains the potency and selectivity of our previously developed cysteine-targeted MSK/RSK inhibitors (Supplemental Table 2), but has increased solubility and stability relative to these compounds (Krishnan et al., 2014; Miller et al., 2013). RMM-64 potently inhibited LPS-induced H3S28ph in primary mouse macrophages, with an IC_{50} <1.0 uM (Figure 3C).

Because RMM-64 also inhibits RSK CTDs, which contain a homologous cysteine, we employed the selective RSK CTD inhibitor FMK to assess the contribution of RSK kinases to LPS-stimulated H3S28 phosphorylation.

Pharmacological inhibition of MSK NTD or CTD but not RSK CTD abolished H3S28ph induction during macrophage stimulation (Figure 3D). RSK inhibition by FMK was confirmed by loss of CTD-dependent internal phosphorylation at S386, and phosphorylation of upstream ERK was unaffected by all agents (Figure 3E–G). Importantly, cell viability and stimulation-dependent phosphorylation of p38, p65 (IKK site), and TBK1 were unaffected or minimally affected by all chemical agents (Figure S3F–G). Our results implicate MSK1/2 as the H3S28 kinases and demonstrate pharmacological inhibition of either the NTD or CTD as an effective strategy for blocking stimulation-dependent H3S28ph.

We favored the temporally incisive use of small molecule inhibitors to study the function of MSK in gene induction during cellular stimulation because this excluded potential effects on roles of MSK1/2 during cellular differentiation and homeostasis. Aware of the potential for off-target effects with chemical agents, we sought rigorous evidence for the role of MSK in H3S28ph while preserving benefits of small-molecule inhibitors. RMM-64 owes its selectivity and affinity to cooperative covalent and non-covalent interactions. The reversible covalent interaction targets a non-catalytic cysteine residue in MSK (MSK1C440, MSK2C425) (Figure 3H). We find that mutation of these cysteines to valines reduces the potency of RMM-64 by approximately 1000-fold and rescues histone H3S28 phosphorylation during LPS stimulation of RAW264.7 macrophages ectopically expressing drug resistant but not wild-type (wt) MSK1/2 (Figure 3H–I, S4).

We next sought to determine the effect of MSK inhibition on H3S28ph induction at specific genomic loci in response to LPS in BMDM. ChIPseq demonstrated abrogation of H3S28ph at the TSS of LPS-induced genes (Figure 3J–K) and at enhancers (Figure 3L) by MSKi but not by RSKi. Together, these results provide evidence that inhibition of H3S28ph by RMM-64 is mediated through its effects on MSK kinases and that MSK is targeted to lineage specific and stimulation responsive chromatin.

MSKs coordinately activate transcription factors and the chromatin template

Identification of MSKs as the principal kinases for H3S28ph at genomic locations enriched for lineage-specific and signal-activated transcription factors led us to consider its previously reported role as an activator of DNA-binding transcription factors. Validating the biological relevance of the transcription factor motif analysis within H3S28ph+ enhancers, with NF-κB/RelA, Creb, and AP-1 among the most enriched (Figure 2E), MSK has been reported to bind to and activate Creb (Deak et al., 1998; Frödin et al., 2002), RelA (Vermeulen et al., 2003) and AP-1 factor, Atf1 (Arthur and Cohen, 2000). Further, these factors have established roles in the inflammatory process (Ananieva et al., 2008; Tong et al., 2016). Consistent with these reports, we found evidence for MSK-dependent activation of transcription factors in stimulated macrophages, with induced phosphorylation of CREB S133 that was reduced following inhibition of MSK with either RMM-64 or SB747651A (Figure 4A–B). Lacking high quality antibodies for p65 S276 phosphorylation, we used an MS-based approach to confirm that MSK1 selectively phosphorylates p65 at S276, a critical

regulatory modification of p65 (Okazaki et al., 2003; Vermeulen et al., 2003) in an *in vitro* kinase assay (Figure 4C–D). This dual role for MSK in the phosphorylation of prominent DNA-binding transcription factors and H3S28 during the stimulation response raised the possibility that MSK kinases could activate transcription factor targets as well as the chromatin template on which they operate, via H3S28ph.

To address the potential for cooperative activation of both chromatin and transcription factors, we developed an *in vitro* transcription assay allowing for assessment of relative contributions of MSK, transcription factor phosphorylation, and histone H3S28 phosphorylation in transcription (Figure 4E). We selected NF-κB (p65/p50; *Rela/Nfkb1*) as a model transcription factor due to its enrichment at H3S28ph chromatin, its role in inflammation, and its potential regulation by MSK (Figure 4C–D). With control over the introduction of MSK1, p300, and NF-κB in the assay and assembly of chromatin with either wt H3 or an H3 mutant (H3S28A) that cannot be phosphorylated at residue 28, we were able to test the function of MSK-mediated phosphorylation of both transcription factor and chromatin template. Using this system, we observed a striking dependence of p65/p50 transcription activity on MSK-mediated phosphorylation and the coordinated activity of MSK targets, H3S28 and NF-κB, on transcription output, with a 2-fold decrease in transcript in the absence of H3S28ph (Figure 4F–G). Therefore, MSK can license both p65/NF-κB and its chromatin template to coordinately augment transcription.

While phosphorylation of p65 and H3S28 were discretely controlled in the NF-κB assays and determined to independently increase transcription, we further sought to evaluate the role of histone phosphorylation in transcription by using an activator that is not regulated by kinase activity. Utilizing a chromatinized template and Gal4-VP16-regulated promoter sequence instead of NF-κB, we found similar increases in p300-dependent transcription on MSK1-phosphorylated chromatin templates (Figure 4H–I). Controlling for the presence of activator (Gal4-VP16), p300, and H3S28ph we again observed a two-fold increase in p300-dependent transcription output in the presence of H3S28ph, but not H3S10ph (Figure 4J–K).

Production of RNA transcript in the *in vitro* chromatin assembly and transcription assay relies on the recruitment and activity of a histone acetyltransferase/coactivator. H3S28ph similarly activated transcription by both p300 and related CBP (Figure 4L). We utilized synthetic H3S28ph or unmodified H3 to establish a role for H3S28ph in p300/CBP-dependent transcription in the absence of MSK (Figure 4L). Consistent with a link between histone phosphorylation and histone acetylation-dependent transcription, we found that the augmented transcription associated with MSK activity was abolished by inhibition of histone acetyl-lysine binding of Brd4 using the inhibitor JQ1 (Figure S5J). Therefore, MSK acts to increase transcription through two distinct downstream mechanisms: 1) through phosphorylation of H3S28 and activation of the chromatin template, and 2) through phosphorylation and increased activity of transcription factors, such as p65. In lieu of methodologies to study the role of H3S28ph directly in cells (due to complexity of mammalian histone genetics), our controlled *in vitro* experiments are suggestive of a cooperative role for transcription factor and chromatin template phosphorylation in cellular responses to stimulation.

H3S28 phosphorylation augments p300 activity

In searching for a potential mechanistic link between H3S28ph and transcriptional activation, we considered previous findings whereby H3S10ph resulted in both recruitment and activation of the HAT GCN5 (Cheung et al., 2000; Clements et al., 2003; Lo et al., 2000). Importantly, H3S10ph occurs within an ARKS motif on the H3 N-terminal tail (Figure 1A), and directs acetylation of regional lysine residues (H3K9 and K14) by GCN5. Given that H3S28 also lies within an ARKS motif, we hypothesized that H3S28ph might similarly augment the recruitment and activity of HAT factors, especially since HS28ph increased p300/CBP-dependent transcription *in vitro*.

Therefore, we investigated the MSK-dependent activity of p300/CBP. H3K27ac can be used as a surrogate of direct p300/CBP recruitment and HAT activity since ~95% of H3K27ac is dependent on p300/CBP (Jin et al., 2011). Supporting H3S28ph-p300/CBP crosstalk, we observed a correlation between sites of rapid H3S28ph accumulation and *de novo* stimulation-dependent H3K27ac increases at promoter and enhancer regions (Figure 5A–B). Stimulation-dependent p300 enrichment was observed at H3S28ph-enriched TSSs, especially among those LPS-response genes characterized by the most prominent increases in H3K27ac (Figure S5A–B). Notably, 88.4% of new or increased H3K27ac “peaks” occurred within regions with significantly enriched levels of H3S28ph (Figure S5C). Further, both H3K27ac and H3S28ph were similarly enriched on nucleosomes flanking transcription factor binding sites that recruit p300 in response to LPS stimulation (Figure 5A).

Given their correlation and kinetic relationship (Figure S5D–E) we investigated the possibility of a more direct role for MSK in acetylation of H3K27 at LPS-response genes. Consistent with a function for MSK and H3S28ph at sites of newly induced H3K27ac, MSK inhibition resulted in a selective decrease in H3K27ac levels at LPS-response genes that were characterized by stimulation-dependent increases in H3K27ac (Figure 5B–C, S5F–G). The effect of MSK inhibition on the overall level of H3K27ac at “pre-activated” LPS-response genes was insignificant (Figure 5C, Figure S5F). Consistent with the observed kinetics of H3S28ph and induced H3K27ac and the positive effect of MSK kinase activity on subsequent H3K27ac, inhibition of p300/CBP had no effect on “upstream” stimulation-dependent H3S28ph (Figure S5H).

We also used established algorithms designed to identify super-enhancers (Whyte et al., 2013) to rank order all macrophage enhancers as well as LPS-induced enhancers. As expected, we found that induced enhancers with the highest H3K27ac signals are associated with prominent macrophage LPS-response genes including *Ccl5, Il27, Nfkbia, and Il12a* (Figure S5I). Overall, MSK inhibition resulted in reduction of H3K27ac levels at LPS-induced enhancers (including induced super enhancers) with little effect on H3K27ac levels at non-induced enhancers (Figure S5H).

Next, we sought to directly test our hypothesis that the phosphorylated ARKS motif at H3S28 might act to recruit and/or activate p300 on the chromatin template, much like phosphorylation of the ARKS motif at H3S10 activates GCN5. Using GST-histone tail pull-down assays (wt-H3, S10A, S28A, S10A/S28A, +/− MSK), we confirmed GCN5

recruitment to H3S10ph. We failed to observe GCN5 binding to H3S28ph (Figure 5D). By contrast, we discovered that recombinant p300 was recruited specifically to H3 tails containing H3S28ph, but not H3S10ph (Figure 5D). We also found that p300 bound preferentially to synthetic H3 peptides bearing H3S28ph but not H3S10ph or unmodified peptides (Figure 5E). Therefore, the specificity of GCN5-H3S10ph and p300-H3S28ph interactions is consistent with a positive effect of ARKS motif phosphorylation on HAT activity at nearby Lys residues (GCN5 at H3K9/14ac, p300 at H3K18/23/27ac). Additionally, p300 recruitment to a chromatinized transcription template was augmented by phosphorylation of H3 by MSK1 (Figure 5F). Importantly, this increased binding was lost under conditions where chromatin was assembled with the H3S28A mutant H3 but not with the H3S10A mutant (Figure 5F). We confirmed that p300 efficiently acetylated MSK1-phosphorylated H3 on chromatinized templates, creating the dual H3K27ac/S28ph modification, using an antibody specific for the H3K27ac/S28ph dual modification (Rothbart et al., 2015) (Figure 5G). LPS stimulation-dependent increases in the dual H3K27ac/S28ph modifications were also observed in BMDM (Figure S1A), further establishing H3 with S28ph as a physiological substrate for p300/CBP.

To better understand the nature of the p300 interaction with H3S28ph, we performed H3 peptide binding assays with p300 domain mutants. These experiments revealed that PHD and Bromo domains are both required for this interaction while the KIX and TAZ domains (the predominant transcription factor interacting domains) appear dispensable (Figure 5H), consistent with a report that PHD, Bromo, and HAT domains form a core domain (Delvecchio et al., 2013). Our data suggest that a feature of this domain facilitates stabilization of p300 on chromatin via H3S28ph. While p300 recruitment to chromatin is mediated predominantly by DNA sequence-specific transcription factors, we propose that H3S28ph also acts directly to stabilize and retain p300 on chromatin.

Chemical inhibition of MSK selectively targets inducible transcription

We considered that MSK kinases integrate upstream signals from p38/MAPK pathways to influence inducible transcription. Thus, we sought to test the effects of inhibiting MSK on induced transcription in stimulated macrophages. To this end, we assessed transcript levels of the most robustly induced LPS-response genes at 60′ and 120′ following LPS stimulation in the presence of MSK inhibitors or a p300/CBP inhibitor (Bowers et al., 2010). Both MSK and p300/CBP inhibition reduced the extent of LPS-stimulated gene induction by an average of ~3-fold at both 60′ and 120′ (Figure 6A, S6A–E). To broadly visualize and assess the selective effects of MSK and p300/CBP inhibition on gene induction, we plotted fold-change and p-value of all genes, comparing control and drug-treated macrophages stimulated with LPS for 60′ (Figure 6B–D). Both MSK inhibitors and the p300 inhibitor selectively reduced the expression of LPS-induced genes compared to all genes ($p<0.0001$) (Figure 6B–D). The marked intersection of genes reduced by 50% or more by the two structurally and mechanistically unrelated MSK inhibitors provides increased confidence in the pharmacological specificity of each inhibitor and indicates that their effects are on-target in the context of LPS-stimulated macrophages (Figure 6E). RNAseq and RT-PCR demonstrated extensive and similar repression of LPS-induced genes by both MSK and p300/CBP inhibition, suggesting linked function in the cellular response (Figure 6F–H).

Consistent with the observed transcriptional changes, secretion of inflammatory factors was markedly reduced by both MSK and p300/CBP inhibition (Figure 6I). Importantly, MSK inhibition resulted in changes in LPS-dependent gene expression that paralleled effects on H3K27ac status (Figure 5B–C): genes with the greatest extent of LPS-induced p300 recruitment and H3K27 acetylation (Figure S5F–G) were also characterized by higher expression levels and greatest sensitivity to MSKi (Figure S6F–G), and p300i (Figure S6H). Increased H3K27ac levels has been causally linked to transcription output (Hilton et al., 2015) thus highlighting the rate-limiting nature of p300 activity and histone acetylation and supporting the importance of an MSK/H3S28ph/p300 pathway for augmented transcription in the rapid cellular response to stimulation.

Discussion

We identified H3S28 phosphorylation as the prominent dynamic histone modification during macrophage stimulation through an unbiased analytical approach. Using pharmacological agents and genetic rescue, we identified MSK1/2 as the primary kinases for this histone modification in macrophages, which marks lineage-specific and stimulation-responsive chromatin, highlighting the role of these kinases in the rapid cellular response to environmental perturbations. From our cellular studies, we conclude that MSKs have an important function in the rapid transcription of inflammatory genes following stimulation of macrophages and that inhibition of MSKs results in selective inhibition of induced transcription. Our mechanistic studies demonstrate, 1) MSK-dependent histone phosphorylation has a direct and positive function in p300/CBP-dependent transcription and that this is a specific feature of phosphorylation at H3S28; and 2) MSKs act coordinately on transcription factors and the chromatin template with additive effects on transcription.

While histone phosphorylation has previously been correlated with gene expression, our study provides evidence for its direct and positive effect on transcription and underscores the fact that H3S10 and H3S28 phosphorylation are not functionally equivalent. Given the conserved role of MSKs in phosphorylation of H3S28 in other cell types (Drobic et al., 2010; Sawicka et al., 2014) and their broad expression profile, there is potential for the mechanisms and function that we describe here in macrophages to feature generally in p38/MAPK-dependent gene regulation.

Dynamic histone acetylation and transcription factor regulation and binding are critical for inflammatory gene induction. p300/CBP recruitment and its HAT activity (at H3K18/K27 and H4) represent critical rate limiting steps in induced transcription as these events precede transcription elongation and are required for nuclear receptor mediated gene induction (Jin et al., 2011). Our study highlights how signaling events can coordinate and precipitate changes in chromatin states and transcription factor activity. We suggest that H3S28ph makes chromatin more permissive to these rate-limiting steps in p300/CBP-dependent transcription. The positive effects of H3S28ph on transcription that we describe here likely cooperate with other known activities of H3S28ph. For example, phosphorylation of H3S28 at repressed chromatin bearing H3K27 methylation could interrupt PRC2-mediated maintenance of heterochromatin (Gehani et al., 2010; Lau and Cheung, 2011) and thereby facilitate derepression and activation of H3K27 methylated genes. We observed an increased

frequency of H3S28ph on the H3 variant H3.3 compared with H3.1/2, perhaps consistent with co-localization of H3S28ph and the H3.3 variant at promoters, enhancers and genic regions. Additional mechanisms for activation of transcription by H3S28ph could include recruitment of 14-3-3 isoforms, SWI/SNF chromatin remodeler, MOF, and PTEF-b (Drobic et al., 2010; Zippo et al., 2009), and also “ejection” of the H3 tail-binding SIN3 corepressor complex (Sawicka et al., 2014).

It will be interesting to determine if H3S28ph has the potential to directly alter the biophysical properties of the chromatin fiber through disruption of electrostatic interactions between the basic H3 tails and negatively charged DNA, as has been reported for some histone acetylations (Müller and Muir, 2015). In support of this possibility, a recent study demonstrated that H3 tail acetylation and phosphorylation, including H3S28ph, increases the accessibility and dynamics of the region surrounding modifications (Stützer et al., 2016). Therefore, H3S28ph may make this region of the H3 tail more permissive to enzyme activity and “reader” binding. It is possible that local H3 tail accessibility plays a role in increased p300/CBP-dependent activity on H3S28 phosphorylated chromatin. We show that H3S28ph delineates stimulation-responsive chromatin neighborhoods containing LPS-induced genes (Figure S2E–F). If induced H3S28ph results in biophysical changes in the chromatin fiber and increased accessibility this may have implications for soluble factor search kinetics, probabilities of regulatory DNA element interactions, and other features occurring within insulated chromatin domains.

In macrophages, the rapid, MSK-dependent accumulation of H3S28ph and subsequent increase in H3K27ac at genomic locations associated with rapidly induced genes is consistent with our biochemical studies linking MSK-dependent transcription factor and histone phosphorylation to p300/CBP-dependent transcription. We suggest that MSKs regulate transcription through dual activation of transcription factors and the chromatin template and that this efficient and coordinated activity is especially critical during rapid cellular responses such as inflammation. Indeed, two-fold differences in transcription are frequently biologically relevant, especially in the context of rapid, *de novo* production of inflammatory mediators (such as Il1, Il6, Ifnb1), chemokines (such as Ccl5, Cxcl1, Cxcl10), and negative regulators of inflammation (such as Nfkbia, Il10, Socs2, Mir155)—all putative MSK regulated genes—and differences within this range of expression are strongly associated with mortality in patients with sepsis and acute respiratory distress syndrome (Carlyn et al., 2015; Meduri et al., 1995). Previous studies have indicated a role for MSKs in induction of anti-inflammatory Il10 in macrophages responding to LPS (Ananieva et al., 2008). Our study indicates a broader activity of MSKs in the expression of both pro- and anti-inflammatory LPS-induced genes. Thus, it will be important to assess how pharmacological inhibition of MSK alters the inflammatory response *in vivo* and the balance between pro- and anti-inflammatory factors that can influence pathology.

A role for MSK in the regulation of inducible transcription prompts consideration of it as a molecular target in the context of dysregulation of inducible transcription in disease. Viable strategies for treatment of both inflammation and cancer include the targeting of disease-associated kinases, including MAPKs and also the inhibition of generic cellular processes, such as acetyl-histone binding and transcription relying on asymmetric effects on pathogenic

processes. MSK1/2, as integrators of ERK and p38 pathway activity, and controllers of multiple downstream transcription mechanisms, represent links between signaling and transcription and appear to selectively control transcription of LPS-induced genes in macrophages. While histone acetyl-lysine binding BET-family members are extensively involved in homeostatic transcription, their targeting with small molecule inhibitors has surprisingly selective effects on inflammatory gene expression (Nicodeme et al., 2010) and oncogenic Myc and its transcriptional program (Delmore et al., 2011). These effects are attributed to the asymmetric dependency on Brd4 of highly expressed genes bearing super enhancers compared with other transcribed genes (Lovén et al., 2013), and their therapeutic use relies critically on these preferential effects over the toxicities associated with reduced Brd4 function in healthy tissues (Bolden et al., 2014). The potential of previous and newly described CDK7/9 inhibitors (Franco and Kraus, 2015) which act through inhibition of transcription, likely rely on similar preferential effects on pathogenic gene product transcription. In contrast, our results point to MSK1/2 as key activators of dual features of *induced* transcription: prominent signal activated transcription factors (including p65 and Creb), and the chromatin template, via H3S28ph. Consistent with this mechanistic understanding of MSK activity, its inhibition, by small molecules that target either the C- or N-terminal kinase domain, appears to selectively reduce the transcription of stimulation-induced genes. Future work that evaluates inhibition of MSK-dependent induced transcription in relevant disease contexts will determine if this selectivity corresponds to improved efficacy and reduced toxicities.

Experimental Procedures

Cell Culture

BMDM were generated from the *in vitro* culture of bone marrow precursor cells isolated from the femurs of C57BL/6 mice (Jackson Laboratories, Bar Harbor, ME) with IL-3 and CSF-1 (5 ng/mL).

Antibody-based methods (flow cytometry and western blotting)

For flow cytometry analysis, BMDM cells were fixed on plates with Foxp3 Fix/Perm staining buffer before staining. For western blotting, cells were first washed with cold PBS before on-plate lysis.

Chromatin Immunoprecipitation

Crosslinking ChIP was performed as described in (Lee et al. 2006) with slight modifications (see Supplemental Experimental Procedures).

Transcription Factor Motif Analysis

Pscan-ChIP was used to determine transcription factor motif enrichment within p300 bound coordinates within and outside-of H3S28ph domains (see Supplemental Experimental Procedures).

RNA-sequencing (RNA-seq) Sample Preparation

RNA was isolated from 1×10^6 or more BMDM cells using the RNeasy Mini Kit (Qiagen, Gaithersburg, MD) and then samples were prepared as instructed using the TruSeq RNA Sample Preparation Kit v2 (Illumina, San Diego, CA).

Genomic Datasets

Genomics data available online, GSE63792: http://www.ncbi.nlm.nih.gov/geo.

Mass Spectrometry Analysis of Histone Post-Translational Modifications

For enrichment of histone phosphorylation TiO_2 columns were used together with synthetic phosphopeptide spike-in for normalization (see Supplemental Experimental Procedures).

Chemical genetics

RAW264.7 macrophages were infected with the PMT2 retroviral vector expressing human MSK1, MSK2, MSK1C440V, or MSK2C425V. Cells were then selected with blasticidin (2.5 ug/mL) and analyzed for H3S28ph by flow cytometry following LPS-stimulation. Uniformly high transgene expressing cells were gated following fixation and permeabilization of cells using anti-HA antibody staining.

Kinase assay

GST-fusion histone and H3/H4 tetramer (500ng) were incubated at 30°C for 1hr with recombinant kinases (100ng of MSK1 and 10ng of active formed pp38) in kinase buffer (10 mM Hepes-KOH, pH 7.9, 100 mM KCl, 10 mM $MgCl_2$, 5% glycerol) containing 10 μM ATP.

In vitro Chromatin assembly

Chromatin was assembled with wt, mutant, and phosphorylated histones (see Supplemental Experimental Procedures).

In vitro transcription assay

Chromatin-based transcription assays were performed as described in (An and Roeder, 2004) (see Supplemental Experimental Procedures).

Cytokine and Chemokine Secretion Assays

BMDM supernatants were analyzed using the Legendplex assay (BioLegend, San Diego, CA) (see Supplemental Experimental Procedures).

Supplementary Material

Refer to Web version on PubMed Central for supplementary material.

Acknowledgments

S.Z.J. is supported by an NIH Pathway to Independence Award (1K99GM113019-01). This work was funded by grants from the NIGMS to C.D.A. (GM040922) and from the NCI (CA129325) and NIDDK (DK071900) to R.G.R.

and from NRF (2014M3A6A4075060, 2011-0020322) to H.P. B.A.G. acknowledges funding from an NIH grant R01GM11017. We thank Koji Hisatake (Tsukuba University, Japan) for providing plasmids of recombinant kinases (MSK1 and pp38). The Proteomics Resource Center at The Rockefeller University acknowledges funding from the Leona M. and Harry B. Helmsley Charitable Trust for mass spectrometer instrumentation. We thank Peter Cheung (York University, Toronto, Canada) for sharing H3 acetyl/phos antibody reagents, Brian D. Strahl and Scott B. Rothbart (University of North Carolina, USA) for testing of antibody specificity and peptide synthesis, Tom W. Muir and Zack Z. Brown (Princeton University, USA) for peptide synthesis, and members of the Allis, Roeder, Muir, and Garcia Laboratories for critical feedback and discussion, especially Ben Sabari, Alexey Soshnev, and Tanya Panchenko.

References

Ananieva O, Darragh J, Johansen C, Carr JM, McIlrath J, Park JM, Wingate A, Monk CE, Toth R, Santos SG, et al. The kinases MSK1 and MSK2 act as negative regulators of Toll-like receptor signaling. Nature Immunology. 2008; 9:1028–1036. [PubMed: 18690222]

Arthur JS, Cohen P. MSK1 is required for CREB phosphorylation in response to mitogens in mouse embryonic stem cells. FEBS Letters. 2000; 482:44–48. [PubMed: 11018520]

Baek SH. When Signaling Kinases Meet Histones and Histone Modifiers in the Nucleus. Molecular Cell. 2011; 42:274–284. [PubMed: 21549306]

Bhatt DM, Pandya-Jones A, Tong AJ, Barozzi I, Lissner MM, Natoli G, Black DL, Smale ST. Transcript Dynamics of Proinflammatory Genes Revealed by Sequence Analysis of Subcellular RNA Fractions. Cell. 2012; 150:279–290. [PubMed: 22817891]

Bolden JE, Tasdemir N, Dow LE, van Es JH, Wilkinson JE, Zhao Z, Clevers H, Lowe SW. Inducible In Vivo Silencing of Brd4 Identifies Potential Toxicities of Sustained BET Protein Inhibition. Cell Reports. 2014; 8:1919–1929. [PubMed: 25242322]

Bowers EM, Yan G, Mukherjee C, Orry A, Wang L, Holbert MA, Crump NT, Hazzalin CA, Liszczak G, Yuan H, et al. Virtual Ligand Screening of the p300/CBP Histone Acetyltransferase: Identification of a Selective Small Molecule Inhibitor. Chemistry & Biology. 2010; 17:471–482. [PubMed: 20534345]

Carlyn CJ, Andersen NJ, Baltch AL, Smith R, Reilly AA, Lawrence DA. Diagnostic Microbiology and Infectious Disease. Diagnostic Microbiology and Infectious Disease. 2015:1–7.

Cheung P, Tanner KG, Cheung WL, Sassone-Corsi P, Denu JM, Allis CD. Synergistic Coupling of Histone H3 Phosphorylation and Acetylation in Response to Epidermal Growth Factor Stimulation. Molecular Cell. 2000; 5:905–915. [PubMed: 10911985]

Clements A, Poux AN, Lo WS, Pillus L, Berger SL, Marmorstein R. Structural Basis for Histone and Phosphohistone Binding by the GCN5 Histone Acetyltransferase. Molecular Cell. 2003; 12:461–473. [PubMed: 14536085]

Deak M, Clifton AD, Lucocq LM, Alessi DR. Mitogen- and stress-activated protein kinase-1 (MSK1) is directly activated by MAPK and SAPK2/p38, and may mediate activation of CREB. The EMBO Journal. 1998; 17:4426–4441. [PubMed: 9687510]

Delmore JE, Issa GC, Lemieux ME, Rahl PB, Shi J, Jacobs HM, Kastritis E, Gilpatrick T, Paranal RM, Qi J, et al. BET Bromodomain Inhibition as a Therapeutic Strategy to Target c-Myc. Cell. 2011; 146:904–917. [PubMed: 21889194]

Delvecchio M, Gaucher J, Aguilar-Gurrieri C, Ortega E, Panne D. Structure of the p300 catalytic core and implications for chromatin targeting and HAT regulation. Nat Struct Mol Biol. 2013

Dowen JM, Fan ZP, Hnisz D, Ren G, Abraham BJ, Zhang LN, Weintraub AS, Schuijers J, Lee TI, Zhao K, et al. Control of cell identity genes occurs in insulated neighborhoods in mammalian chromosomes. Cell. 2014; 159:374–387. [PubMed: 25303531]

Drobic B, Pérez-Cadahía B, Yu J, Kung SKP, Davie JR. Promoter chromatin remodeling of immediate-early genes is mediated through H3 phosphorylation at either serine 28 or 10 by the MSK1 multi-protein complex. Nucleic Acids Research. 2010; 38:3196–3208. [PubMed: 20129940]

Franco HL, Kraus WL. No Driver behind the Wheel? Targeting Transcription in Cancer. Cell. 2015; 163:28–30. [PubMed: 26406367]

Frödin M, Antal TL, Dümmler BA, Jensen CJ, Deak M, Gammeltoft S, Biondi RM. A phosphoserine/threonine-binding pocket in AGC kinases and PDK1 mediates activation by hydrophobic motif phosphorylation. The EMBO Journal. 2002; 21:5396–5407. [PubMed: 12374740]

Gehani SS, Agrawal-Singh S, Dietrich N, Christophersen NS, Helin K, Hansen K. Polycomb Group Protein Displacement and Gene Activation through MSK-Dependent H3K27me3S28 Phosphorylation. Molecular Cell. 2010; 39:886–900. [PubMed: 20864036]

Hargreaves DC, Horng T, Medzhitov R. Control of Inducible Gene Expression by Signal-Dependent Transcriptional Elongation. Cell. 2009; 138:129–145. [PubMed: 19596240]

Hilton IB, D'Ippolito AM, Vockley CM, Thakore PI, Crawford GE, Reddy TE, Gersbach CA. Epigenome editing by a CRISPR-Cas9-based acetyltransferase activates genes from promoters and enhancers. Nat Biotechnol. 2015; 33:510–517. [PubMed: 25849900]

Jin Q, Yu LR, Wang L, Zhang Z, Kasper LH, Lee JE, Wang C, Brindle PK, Dent SYR, Ge K. Distinct roles of GCN5/PCAF-mediated H3K9ac and CBP/p300-mediated H3K18/27ac in nuclear receptor transactivation. The EMBO Journal. 2011; 30:249–262. [PubMed: 21131905]

Krishnan S, Miller RM, Tian B, Mullins RD, Jacobson MP, Taunton J. Design of reversible, cysteine-targeted Michael acceptors guided by kinetic and computational analysis. J Am Chem Soc. 2014; 136:12624–12630. [PubMed: 25153195]

Lau PNI, Cheung P. Histone code pathway involving H3 S28 phosphorylation and K27 acetylation activates transcription and antagonizes polycomb silencing. Proceedings of the National Academy of Sciences of the United States of America. 2011; 108:2801–2806. [PubMed: 21282660]

Lo WS, Trievel RC, Rojas JR, Duggan L, Hsu JY, Allis CD, Marmorstein R, Berger SL. Phosphorylation of Serine 10 in Histone H3 Is Functionally Linked In Vitro and In Vivo to Gcn5-Mediated Acetylation at Lysine 14. Molecular Cell. 2000; 5:917–926. [PubMed: 10911986]

Lovén J, Hoke HA, Lin CY, Lau A, Orlando DA, Vakoc CR, Bradner JE, Lee TI, Young RA. Selective Inhibition of Tumor Oncogenes by Disruption of Super-Enhancers. Cell. 2013; 153:320–334. [PubMed: 23582323]

Mahadevan LC, Willis AC, Barratt MJ. Rapid histone H3 phosphorylation in response to growth factors, phorbol esters, okadaic acid, and protein synthesis inhibitors. Cell. 1991; 65:775–783. [PubMed: 2040014]

Meduri GU, Headley S, Kohler G, Stentz F, Tolley E, Umberger R, Leeper K. Persistent elevation of inflammatory cytokines predicts a poor outcome in ARDS. Plasma IL-1 beta and IL-6 levels are consistent and efficient predictors of outcome over time. Chest. 1995; 107:1062–1073. [PubMed: 7705118]

Miller RM, Paavilainen VO, Krishnan S, Serafimova IM, Taunton J. Electrophilic Fragment-Based Design of Reversible Covalent Kinase Inhibitors. J Am Chem Soc. 2013; 135:5298–5301. [PubMed: 23540679]

Müller MM, Muir TW. Histones: at the crossroads of peptide and protein chemistry. Chem Rev. 2015; 115:2296–2349. [PubMed: 25330018]

Naqvi S, Macdonald A, McCoy CE, Darragh J, Reith AD, Arthur JSC. Characterization of the cellular action of the MSK inhibitor SB-747651A. Biochem J. 2012; 441:347–357. [PubMed: 21970321]

Nicodeme E, Jeffrey KL, Schaefer U, Beinke S, Dewell S, Chung CW, Chandwani R, Marazzi I, Wilson P, Coste H, et al. Suppression of inflammation by a synthetic histone mimic. Nature. 2010; 468:1119–1123. [PubMed: 21068722]

Okazaki T, Sakon S, Sasazuki T, Sakurai H, Doi T, Yagita H, Okumura K, Nakano H. Phosphorylation of serine 276 is essential for p65 NF-kappaB subunit-dependent cellular responses. Biochem Biophys Res Commun. 2003; 300:807–812. [PubMed: 12559944]

Ostuni R, Piccolo V, Barozzi I, Polletti S, Termanini A, Bonifacio S, Curina A, Prosperini E, Ghisletti S, Natoli G. Latent enhancers activated by stimulation in differentiated cells. Cell. 2013; 152:157–171. [PubMed: 23332752]

Ramirez-Carrozzi VR, Braas D, Bhatt DM, Cheng CS, Hong C, Doty KR, Black JC, Hoffmann A, Carey M, Smale ST. A Unifying Model for the Selective Regulation of Inducible Transcription by CpG Islands and Nucleosome Remodeling. Cell. 2009; 138:114–128. [PubMed: 19596239]

Rothbart SB, Dickson BM, Raab JR, Grzybowski AT, Krajewski K, Guo AH, Shanle EK, Josefowicz SZ, Fuchs SM, Allis CD, et al. An Interactive Database for the Assessment of Histone Antibody Specificity. Molecular Cell. 2015; 59:502–511. [PubMed: 26212453]

Sawicka A, Hartl D, Goiser M, Pusch O, Stocsits RR, Tamir IM, Mechtler K, Seiser C. H3S28 phosphorylation is a hallmark of the transcriptional response to cellular stress. Genome Res. 2014

Stützer A, Liokatis S, Kiesel A, Schwarzer D, Sprangers R, Söding J, Selenko P, Fischle W. Modulations of DNA Contacts by Linker Histones and Post-translational Modifications Determine the Mobility and Modifiability of Nucleosomal H3 Tails. Molecular Cell. 2016

Thomson S. The nucleosomal response associated with immediate-early gene induction is mediated via alternative MAP kinase cascades: MSK1 as a potential histone H3/HMG-14 kinase. The EMBO Journal. 1999; 18:4779–4793. [PubMed: 10469656]

Tong AJ, Liu X, Thomas BJ, Lissner MM, Baker MR, Senagolage MD, Allred AL, Barish GD, Smale ST. A Stringent Systems Approach Uncovers Gene-Specific Mechanisms Regulating Inflammation. Cell. 2016; 165:165–179. [PubMed: 26924576]

Vermeulen L, De Wilde G, Van Damme P, Vanden Berghe W, Haegeman G. Transcriptional activation of the NF-kappaB p65 subunit by mitogen- and stress-activated protein kinase-1 (MSK1). The EMBO Journal. 2003; 22:1313–1324. [PubMed: 12628924]

Whyte WA, Orlando DA, Hnisz D, Abraham BJ, Lin CY, Kagey MH, Rahl PB, Lee TI, Young RA. Master Transcription Factors and Mediator Establish Super-Enhancers at Key Cell Identity Genes. Cell. 2013; 153:307–319. [PubMed: 23582322]

Zippo A, Serafini R, Rocchigiani M, Pennacchini S, Krepelova A, Oliviero S. Histone Crosstalk between H3S10ph and H4K16ac Generates a Histone Code that Mediates Transcription Elongation. Cell. 2009; 138:1122–1136. [PubMed: 19766566]

Highlights

- H3S28 phosphorylation (H3S28ph) is a dominant stimulation-dependent modification
- MSKs phosphorylate both H3S28 and transcription factors with additive effects
- MSKs and H3S28ph selectively increase p300-dependent transcription
- Chemical inhibition of MSKs selectively targets inducible transcription

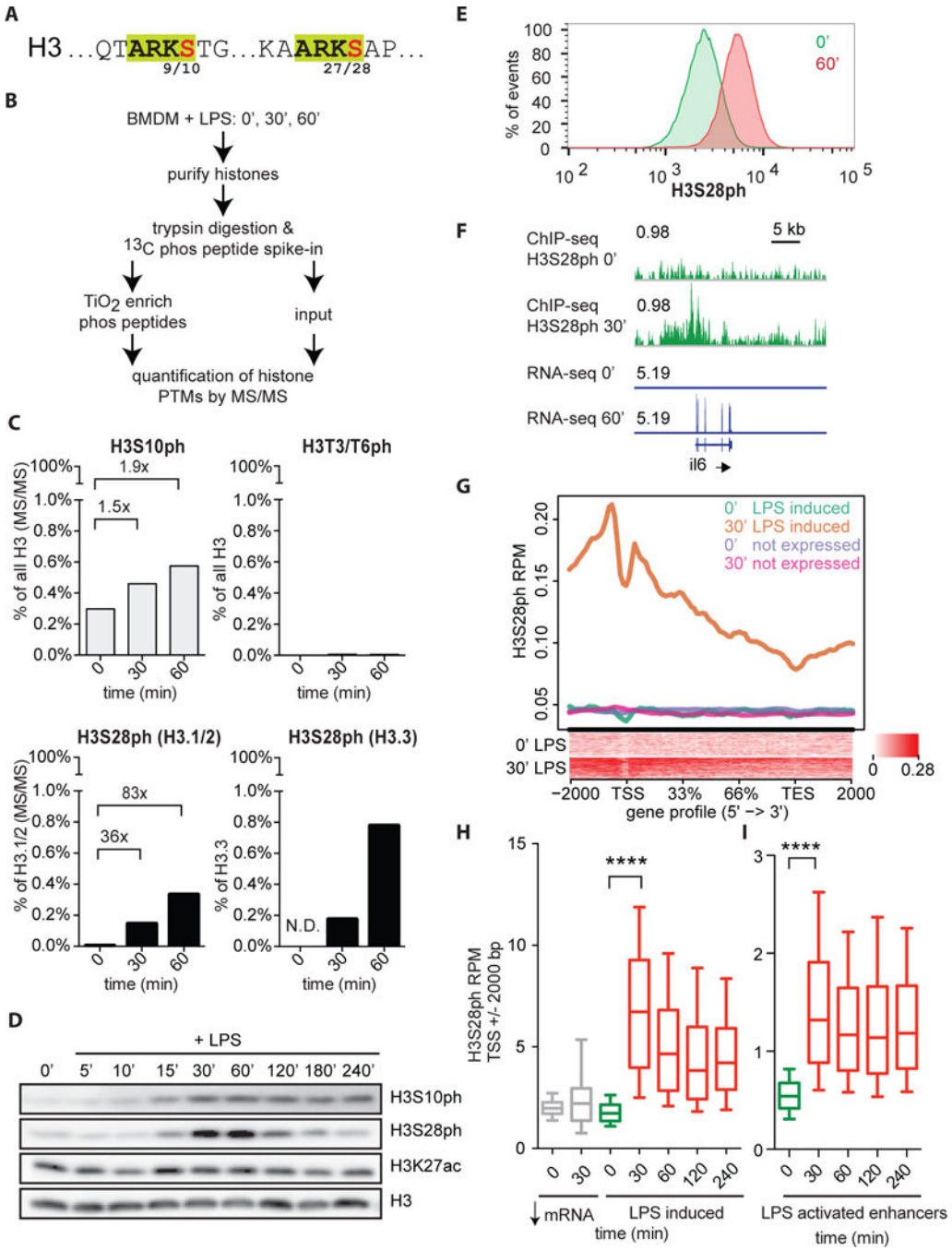

Figure 1. Dynamic H3S28 phosphorylation foot-prints chromatin-associated kinase activity in stimulated mouse macrophages

(A) N-terminal tail of histone H3 with ARKS motifs highlighted in green and key serine residues in red.

(B) Experimental design for quantification of histone phosphorylation events during BMDM stimulation by MS/MS.

(C) MS/MS quantification of H3S10ph (upper left), H3T3 or H3T6p (upper right) on all H3 variants; H3S28ph on H3.1/2 variants (lower left), and H3S28ph on H3.3 variant (lower right), at 0, 30, and 60 minutes from BMDM following LPS stimulation. Fold increase

compared to unstimulated condition (0′) is shown above bar graphs where 0′ was detectible. N.D., not detected. Representative of two separate experiments.

(D) Western blot analysis of histone modifications throughout the BMDM response to LPS. Numbers above lanes represent minutes following LPS addition.

(E) Flow cytometric analysis of population-level H3S28ph at 0 and 60 minutes following LPS stimulation of BMDM.

(F) Representative ChIPseq data for stimulation-dependent increase in H3S28ph at induced inflammatory genes. From top to bottom: H3S28ph ChIPseq 0′; H3S28ph ChIPseq 30′; RNAseq 0′; RNAseq 60′; refseq gene track information for il6. y-axis scale (tag density) is indicated on each track.

(G) Average H3S28ph ChIPseq gene profiles for LPS-induced genes (by RNAseq, 336 isoforms, RPKM>1, induced >5-fold at 60′ LPS exposure, heat maps below) and not expressed genes (RPKM 0) at 0′ and 30′ following LPS stimulation.

(H–I) Median and distribution (box, quartiles; whiskers, 90th-percentile) of H3S28ph RPM/RPKM values for (H) transcription start sites (TSS) +/− 2000bp at not-expressed genes (down-arrow, mRNA), and LPS-induced genes or (I) poised, LPS-activated enhancers throughout the stimulation response of BMDM to LPS.

Results are representative of two or more experiments.

See also Figure S1.

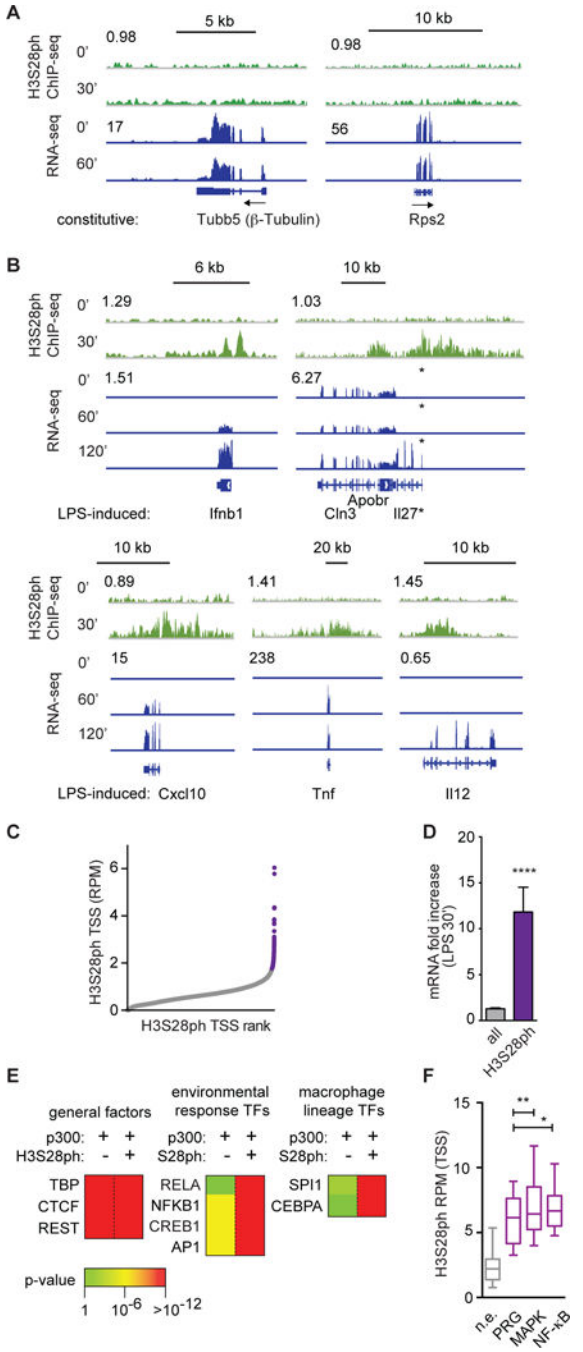

Figure 2. H3S28 phosphorylation is targeted to lineage-specific and stimulation-responsive chromatin

(A–B) H3S28ph ChIPseq (0′, 30′ - peak of signal) and RNAseq (0′, 60′) profiles in LPS-stimulated bone marrow derived macrophages for (A) constitutively expressed genes, Tubb5 and Rps2, and (B) LPS-induced Ifnb1, Il27, Cxcl10, Tnf, Il12a (also with 120′ RNAseq) with y-axis scale (tag density) indicated.

(C) All genes were ranked by H3S28ph signal density (RPM) at their TSS+/− 2kb. A threshold for the top H3S28ph genes, purple, was empirically determined based on ChIPseq signal over background (RPM>1.83).

(D) Fold change in mRNA following LPS treatment for all genes (gray) or top H3S28ph genes (purple, RPM>1.83). $p<0.0001$, Student's t-test.
(E) Heat map displaying p-values of highly enriched transcription factor (TF) motifs from three categories: general (control) TFs (left), environmental response TFs (middle), macrophage lineage specifying TFs (right), for H3S28ph-positive (overlap of p300 and H3S28ph enriched regions) and –negative (p300 enriched sites lacking H3S28ph enrichment) enhancers. Enhancer coordinates were analyzed with Pscan-ChIP (see methods).
(F) H3S28ph ChIPseq signal (RPM) around the TSS (+/− 2kb) of genes that are not expressed (n.e.), primary response genes (PRG), MAPK-dependent genes, and NF-κB-dependent genes (NF-κB). Gene lists derived from Tong et al., 2016. Mean, std dev., 95% CI, with $p<0.01$ (**) and $p<0.05$ (*), Student's t-test.
See also Figure S2.

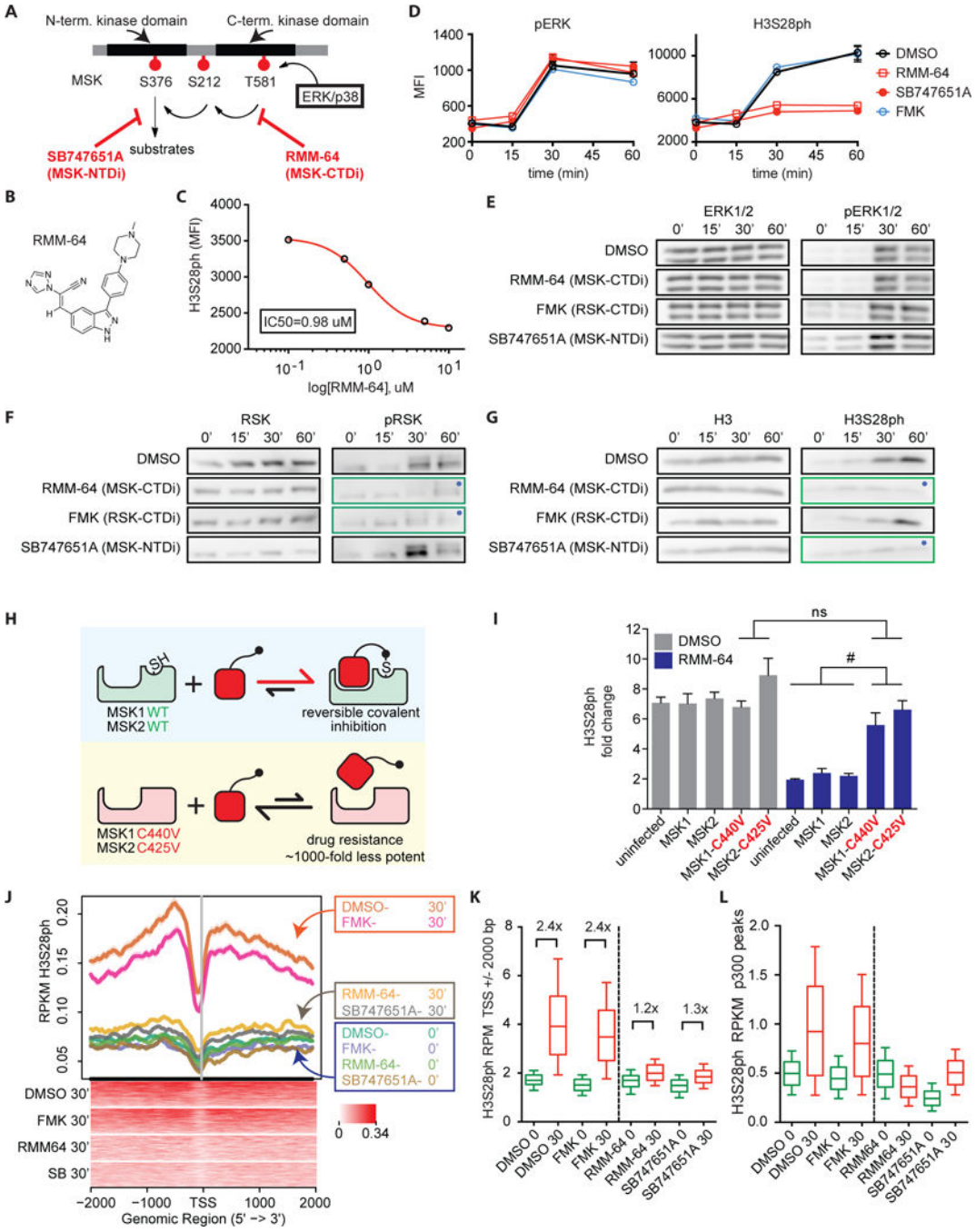

Figure 3. Mitogen- and stress-activated kinases signal to inflammatory genes in chromatin

(A) Schematic of MSK kinase domain organization, phosphorylation sites, and activities of CTD and NTD inhibitors, RMM-64 and SB747651A, respectively.

(B) RMM-64; systematic (IUPAC) name: 3-(3-(4-(4-methylpiperazin-1-yl)phenyl)-1H-indazol-5-yl)-2-(1H-1,2,4-triazol-1-yl)acrylonitrile.

(C) H3S28ph antagonist dose-response curve for determination of half maximal inhibitory concentration (IC_{50}) of RMM-64 in BMDM. IC_{50}=0.98 uM. H3S28ph levels (mean fluorescence intensity, MFI) were determined by quantitative flow cytometry.

(D) Effects of pharmacological inhibition of MSK-CTD, MSK-NTD (MSK-CTDi—RMM-64, 5 uM and MSK-NTDi—SB747651A, 5 uM), and RSK (RSK-CTDi—FMK, 5 uM) on pERK1/2 and H3S28ph during stimulation of BMDM with LPS by quantitative flow cytometry.

(E–G) Western blot characterization of effects of RMM-64 (5 uM), FMK (5 uM), SB747651A (5 uM) on (E) pERK (control), (F) internal C-term. RSK S380p and (G) H3S28ph in BMDM. Loading controls: ERK1/2, histone H3, RSK. Blue dots indicate expected inhibitory effects on putative targets of chemical agents.

(H) Model for mechanism of reversible covalent inhibitor (RMM-64) targeting of non-catalytic cysteine residues and the experimental approach to MSK1/2 chemical genetics experiments.

(I) Fold change (LPS-dependent increase) in H3S28ph in RAW264.7 macrophages expressing wt or RMM-64 resistant MSK mutants (MSK1-C440V, MSK2-C425V), as measured by quantitative flow cytometry.

(J) H3S28ph ChIPseq average profiles at LPS-induced gene TSS +/− 2000 bp at 0′ and 30′ following LPS stimulation under the indicated drug treatment conditions in BMDM (as in D–G).

(K–L) H3S28ph RPM median and distribution (quartiles and 90th percentile) at (K) TSS of LPS-induced genes +/− 2000bp and (L) p300 peaks in BMDM. Fold increase compared to unstimulated condition (0′) is shown above whisker plots; stimulation resulted in significant increases in RPM values for all conditions, $p<0.0001$, paired t-test. Data are representative of three or more experiments (C–I), with the exception of H3S28ph ChIPseq with pharmacological agents (J–L, single experiment).

See also Figure S3 and S4.

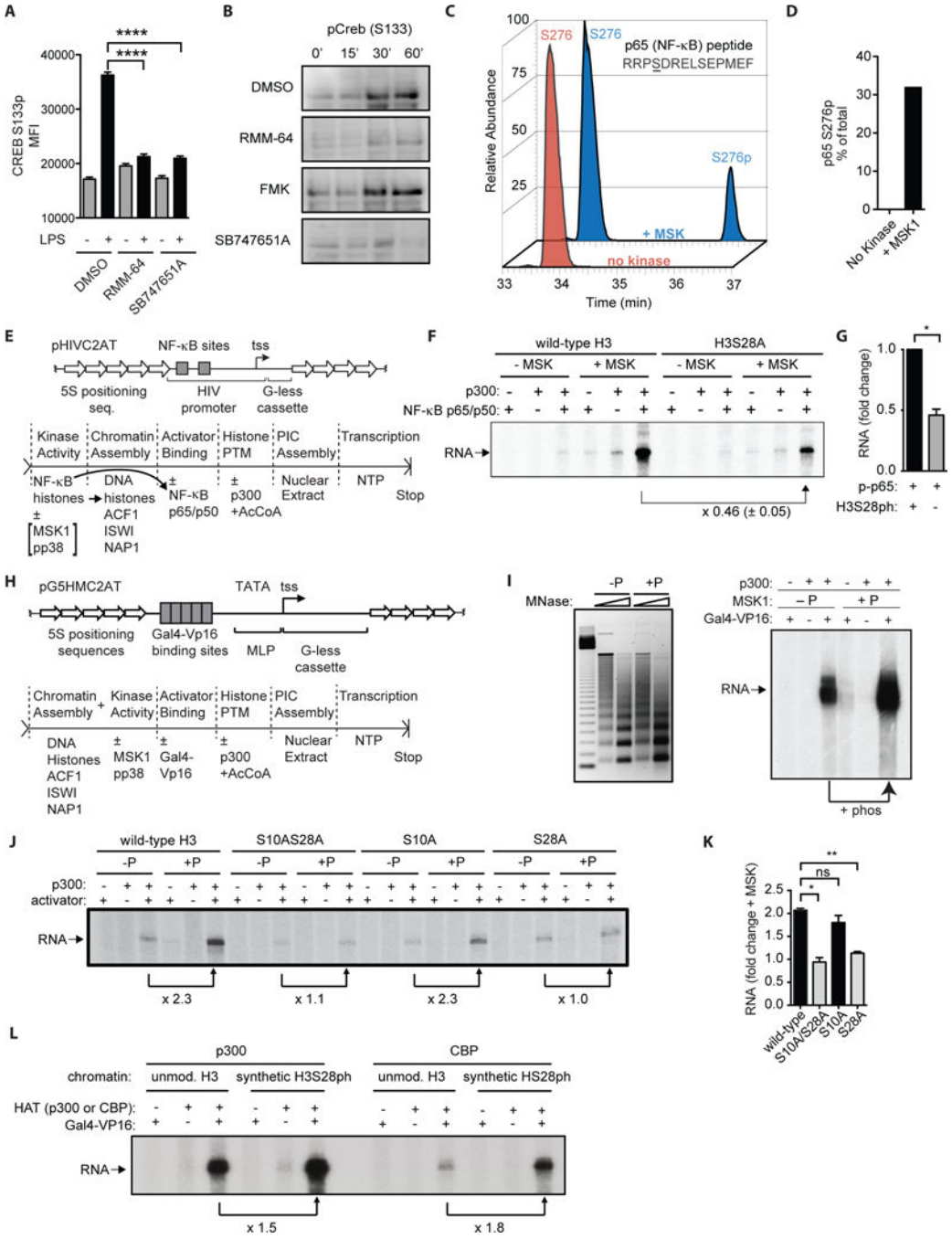

Figure 4. MSK coordinately activates NF-κB and the chromatin template via H3S28 phosphorylation, with additive effects on p300/CBP-dependent transcription

(A–B) Effects of pharmacological inhibition of MSK on Creb S133p during stimulation of BMDM with LPS for 30′ by (A) quantitative flow cytometry and (B) western blot analysis. (C) Extracted ion chromatograms (XIC) from mass spectrometry data for p65 peptide RRPS^{276}DRELSEPMEF, with or without S276 phosphorylation, summing signals for doubly and triply charged ions. The XIC demonstrates no signal for the phosphorylated peptide in the untreated sample and enrichment of the phosphorylated peptide in the +MSK1 condition.

(D) Quantitation of p65 S276p stoichiometry in control and MSK treated p65 based on MS signals of summed doubly and triply charged ions. Representative of two separate experiments.

(E) Schematic of the template DNA construction (pHIVC2AT) and procedure for NF-κB-mediated *in vitro* transcription assay.

(F–G) *In vitro* transcription assay with NF-κB p65/p50 as activator and p300 as coactivator and using chromatin templates assembled with either wt H3 or H3S28A mutants. (G) Band density (RNA) was measured with densitometry and the ratio in signal between wt and H3S28A mutant for two experiments is shown, with error bars indicated standard deviation. rMSK1 was used to phosphorylate histones (+MSK) assembled into chromatin.

(H) Schematic of the experimental procedure for the Gal4-Vp16 *in vitro* transcription assay.

(I) *In vitro* transcription assay on chromatinized template using the Gal4-VP16 activator and p300 as co-activator. rMSK1 was used to phosphorylate histones (+P) assembled into chromatin. Left, chromatin integrity as assessed by MNase digestion of control (−P) and MSK treated (+P) chromatin templates. Right, autoradiograph of the RNA transcript is shown.

(J) *in vitro* transcription assay, as in (I), with wt and H3 serine-to-alanine mutants: H3S10A/S28A; H3S10A; H3S28A.

(K) Autoradiograph RNA signal from (J) was quantified by densitometry. Error bars indicate standard deviation of 2 replicates.

(L) Synthetic H3, either unmodified or containing S28ph, was used in place of recombinant H3 for chromatin assembly and transcription assays, as in (I–J) using either p300 or CBP as coactivator.

Autoradiograph RNA signals were quantified by densitometry. Arrows indicate fold change with MSK1 kinase activity or synthetic histone phosphorylation. All results are representative of two or more experiments.

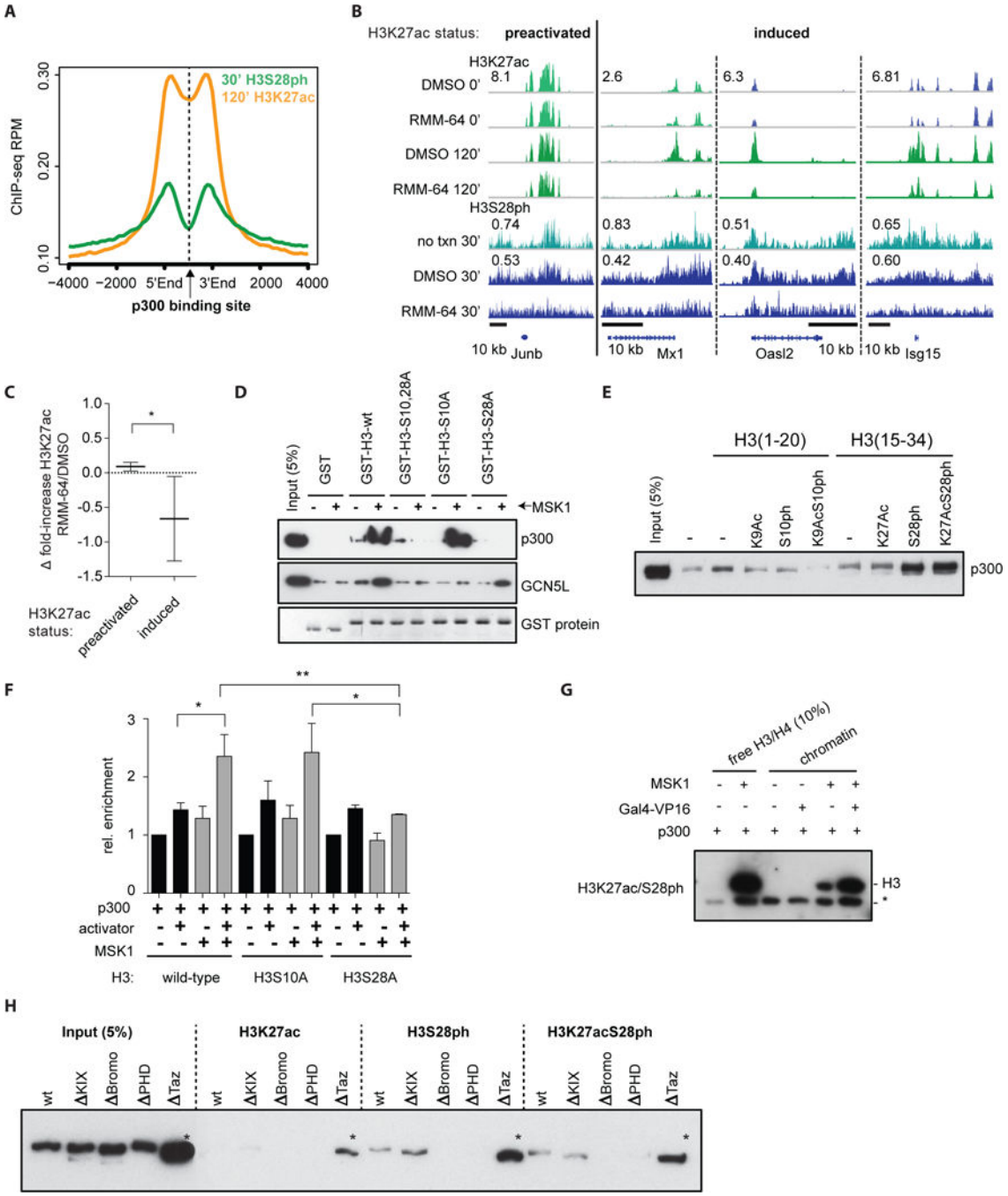

Figure 5. H3S28 phosphorylation augments p300 activity

(A) H3S28ph and H3K27ac ChIP average profile around p300-binding sites in LPS-stimulated (H3S28ph- 30′, H3K27ac- 120′) BMDM.

(B) H3S28ph and H3K27ac ChIPseq results at representative preactivated (LPS-response genes with <2-fold increase in H3K27ac at TSS +/− 2kb at 120′) or induced genes (>2-fold increase in H3K27ac) in untreated, RMM-64, or DMSO treated BMDM, unstimulated (0′) and LPS-stimulated (30′- H3S28ph; 120′-H3K27ac; at the peak of their respective signals),

demonstrating de novo H3K27ac peaks within H3S28ph regions and effects of MSK inhibition on H3S28ph and H3K27ac.

(C) Ratio of LPS-induced fold increase of H3K27ac between RMM-64 and DMSO treated BMDM at all preactivated (little to no change in H3K27ac) or induced (>2-fold increase in H3K27ac) genes. Error bars indicate standard deviation, *, p-value<0.05.

(D) p300 and GCN5L pull-down assays using recombinant GST-H3 (residues 1–40) proteins bearing either wt or mutated (S10A alone, S28A alone, or S10A/S28A together) H3 sequences and either untreated (−) or phosphorylated with rMSK1 (+). (E) synthetic biotinylated histone tail peptide pull-downs for p300 with the indicated histone modifications.

(F) "*in vitro* ChIP" assay, wherein recruitment of chromatinized template to p300-bound beads was determined by qPCR under various conditions (activator, Gal4-VP16; chromatin template pre-treated with rMSK1; wt or H3 serine mutants, H3S10A or H3S28A).

(G) Western blot analysis of p300 histone acetyltransferase assays on chromatinized template substrate, using an antibody that selectively recognizes the combinatorial K-ac/S-ph motif (K27ac/S28ph). *, a nonspecific band.

(H) Synthetic biotinylated histone peptide pull-downs (histone H3 N-terminal tail, residues 15–35) with recombinant full length or domain mutant p300 protein. 5% input is shown. * - high expression/background for Taz mutant construct.

See also Figure S5.

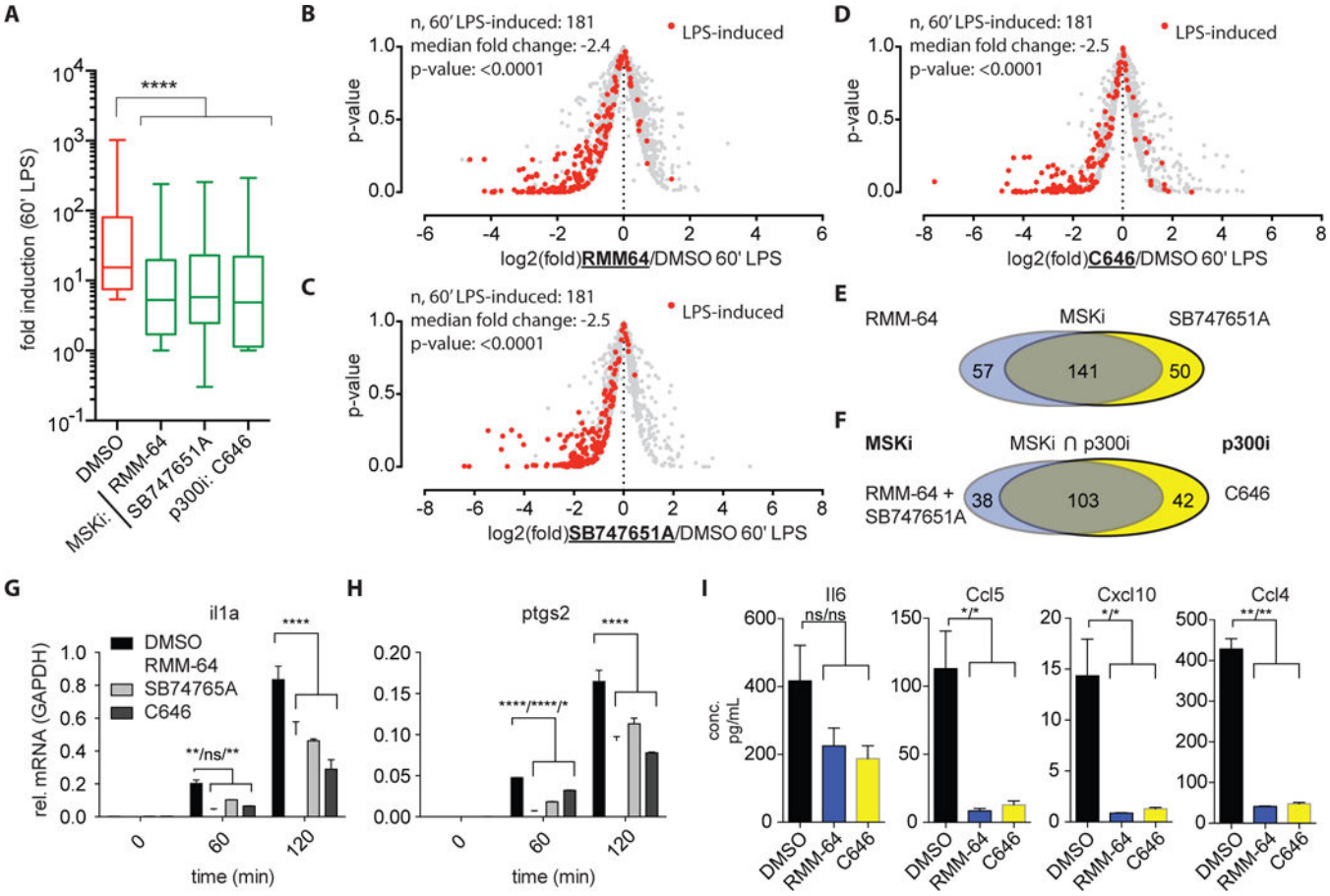

Figure 6. MSK inhibition selectively targets inducible transcription

(A) RNAseq fold-induction of LPS-induced genes from 0′ to 60′ following BMDM stimulation in the presence of DMSO (control), MSK-CTDi (RMM-64, 5 uM), MSK-NTDi (SB747651A, 5 uM), or p300i (C646, 37.5 uM). Median and distribution (box, quartiles; whiskers, 90th-percentile) are shown. ****, p-value<0.0001.

(B–D) Scatter plot of log2 fold change of 60′ LPS stimulated BMDM under three treatment conditions: (B) MSK inhibitor RMM-64, 5 uM; (C) MSK inhibitor SB747651A, 5 uM; (D) p300 inhibitor, C646, 37.5 uM. LPS-induced genes, independently assessed, are visualized in red, with all other genes in grey. Shown for each condition (B–D) are median fold change of LPS-induced genes and p-value, student t-test comparing change in LPS-induced genes to all genes.

(E) Convergence of genes reduced by 50% or more by both MSK inhibitors (RMM-64 and SB747651A), among LPS-induced genes (>5-fold increase, FPKM>1, 60′ stimulation).

(F) Convergence of genes repressed by 50% or more by both MSKi conditions (141 genes from (E)) and C646 (p300i), among LPS-induced genes.

(G–H) RT-qPCR validation is shown for two representative LPS-response genes affected by both MSK and p300 inhibition; (G) Il1a and (H) Ptgs2.

(I) Secreted inflammatory mediator protein abundance in BMDM cell supernatants from control (DMSO), RMM-64 (MSKi), and C646 (p300i) treatment conditions following stimulation with LPS for 3 hours.